Power Allocation for Beamforming Relay Networks under Channel Uncertainties

Jingon Joung and Ali H. Sayed
Department of Electrical Engineering
University of California (UCLA)
Los Angeles, CA 90095, USA.
Emails: {jgjoung, sayed}@ee.ucla.edu

***Abstract*—Under uncertain channel conditions, local and global power control factors for amplify-and-forward relay processing and source-destination beamforming are jointly and iteratively designed based on a minimum mean-square-error (MMSE) criterion. The influence of imperfect channel information on system performance is examined by computer simulation. As a result, it is verified that the proposed power control methods can relieve the performance degradation arising from channel uncertainties.**

I. Introduction

Power allocation strategies have attracted considerable attention in an effort to reduce the network power and/or improve the performance of the cooperative relay networks [1]–[4]. In cooperative relay networks, multiple relays cooperate to retransmit data. In [2], power control factors are designed to maximize a signal-to-noise ratio (SNR) upper bound. Under the assumption that the source node uses some reasonable fraction of the total network power, optimal allocation of the remaining power among the relay nodes was found to maximize the throughput and minimize the outage probability [3]. In addition, minimum global power design under the SNR constraint was considered in [4].

For single relay networks, power allocation methods have also been studied as an important part of the relay system design. Various multiple-input multiple-output (MIMO) techniques can be implemented with a single relay having multiple antennas. Among them, beamforming provides array and diversity gain at the cost of knowing the channel state information (CSI) at both the transmitter and receiver. The optimal beamforming and relay processing tasks have been realized in [6] by maximizing the received SNR with perfect CSI at every node. In the mean time, *local equality* transmit power constraints on the source and the relay were considered. In the local equality power constraint case, transmit power at the source and the relay is fixed by its own maximum available power. To mitigate the burden of full CSI at the transmitters, a codebook-based beamforming and antenna selection method, which is a special case of beamforming, have been proposed [5], [6].

This work was supported in part by NSF grants ECS-0601266 and ECS-0725441 and by the Korea Research Foundation Grant funded by the Korean Government [KRF-2008-357-D00179].

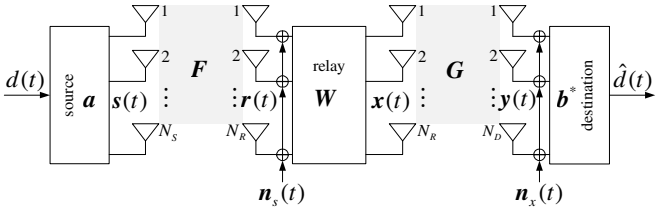

Fig. 1. Two-hop amplify-and-forward MIMO relay system model with one source and one destination nodes.

In this paper, we focus on the beamforming relay networks as in [6] and propose power allocation methods to minimize mean-square-error (MSE) under imperfect CSI conditions. In this minimum MSE (MMSE) optimization, we consider *local* and *global inequality* power constraints at both the source and the relay. In the local inequality power constraint case, the transmit power at the source and the relay is locally bounded instead of being fixed. In the global power constraint case, the network power for the source and the relay in half-duplex mode is globally bounded. For the beamforming, we adopt scaled eigen beamforming at each node similar to [6]. The scaling factors perform power adjustment in relay networks. Accordingly, the MMSE-based design for the optimal beamforming vectors and relay processing matrix become identical to the MMSE-based design for the optimal *power control factors* in the equivalent single-input single-output (SISO) relay network model. Following an alternating optimization procedure, where variables are optimized one at a time while keeping all others fixed [7], [8], closed form Karush-Kuhn-Tucker (KKT) conditions [9] are derived, and iterative algorithms are then developed with the entangled KKT equalities to achieve MMSE performance. Computer simulation illustrates that performance degradation arising from the channel uncertainties can be reduced by the proposed beamforming.

Notation. Throughout this paper, for any vector or matrix, the superscript '$*$' denotes complex conjugate transposition. $\boldsymbol{I}_q$ is a q-dimensional identity matrix; $\mathrm{Re}(\cdot)$ represents the real part; for any scalar q and vector $\boldsymbol{q}$, the notations $|q|$ and $\|\boldsymbol{q}\|$ denote the absolute value of q and 2-norm of $\boldsymbol{q}$, respectively; and 'E' stands for expectation of a random variable.

978-1-4244-4148-8/09/$25.00 ©2009

II. Relay System and Signal Model

A two-hop half-duplex beamforming relay system model is shown in Fig. 1. The source, relay, and destination nodes have N_S, N_R, and N_D antennas, respectively, where N_S and N_D are greater than or equal to two for beamforming purpose while $N_R \geq 1$. For convenience of illustration, the relay is shown with separate transmit and receive antennas. Direct path from the source to the destination in this model is not considered in this paper [10]. The channel matrices of the first- and second-hops are represented by $\boldsymbol{F} \in \mathbb{C}^{N_R \times N_S}$ and $\boldsymbol{G} \in \mathbb{C}^{N_D \times N_R}$, respectively. The elements of $\boldsymbol{F}$ and $\boldsymbol{G}$ are independent and identically distributed (i.i.d) and zero-mean complex Gaussian random variables with unit variance without loss of generality. Path loss from the effects of shadowing and large scale fading can be taken into account by adjusting the noise variance at the receiver side. It is assumed that every channel remains static during one data block (or frame) transmission. Data symbols at time t are denoted by $d(t)$, whose average power over time $\mathrm{E}\,|d(t)|^2 = 1$, so that the transmitted symbol vector from the source is given by

$$\boldsymbol{s}(t) = \boldsymbol{a}d(t) \in \mathbb{C}^{N_S \times 1} \tag{1}$$

where $\boldsymbol{a} \in \mathbb{C}^{N_S \times 1}$ is a transmit beamforming vector. Through the first-hop, the received signal vector at the relay is

$$\boldsymbol{r}(t) = \boldsymbol{F}\boldsymbol{s}(t) + \boldsymbol{n}_s(t) \in \mathbb{C}^{N_R \times 1} \tag{2}$$

where $\boldsymbol{n}_s(t) \in \mathbb{C}^{N_R \times 1}$ is a zero-mean additive white Gaussian noise (AWGN) vector and $\mathrm{E}\,\boldsymbol{n}_s(t)\boldsymbol{n}_s^*(t) = \sigma_{n_s}^2 \boldsymbol{I}_{N_R}$. The relay multiplies $\boldsymbol{r}(t)$ by the relay processing matrix $\boldsymbol{W} \in \mathbb{C}^{N_R \times N_R}$, and forwards $\boldsymbol{x}(t) \in \mathbb{C}^{N_R \times 1}$ through the second-hop, where

$$\boldsymbol{x}(t) = \boldsymbol{W}\boldsymbol{r}(t). \tag{3}$$

At the destination, the received signal vector is

$$\boldsymbol{y}(t) = \boldsymbol{G}\boldsymbol{x}(t) + \boldsymbol{n}_x(t) \in \mathbb{C}^{N_D \times 1} \tag{4}$$

where $\boldsymbol{n}_x(t) \in \mathbb{C}^{N_D \times 1}$ is an AWGN vector and $\mathrm{E}\,\boldsymbol{n}_x(t)\boldsymbol{n}_x^*(t) = \sigma_{n_x}^2 \boldsymbol{I}_{N_D}$. The destination combines the received signal as follows:

$$\hat{d}(t) = \boldsymbol{b}^*\boldsymbol{y}(t) \tag{5}$$

by using a receive beamforming vector $\boldsymbol{b}^* \in \mathbb{C}^{1 \times N_D}$. For simplicity, the time index t is henceforth omitted whenever convenient.

III. Eigen Beamforming with CSI Uncertainties

Using (1)–(5), the overall signal model can be written as

$$\hat{d} = \boldsymbol{b}^*\boldsymbol{G}\boldsymbol{W}\boldsymbol{F}\boldsymbol{a}d + \boldsymbol{b}^*\boldsymbol{G}\boldsymbol{W}\boldsymbol{n}_s + \boldsymbol{b}^*\boldsymbol{n}_x. \tag{6}$$

By employing eigen beamforming at each node [6], we define the beamforming vectors and relay processing matrix in (6) as:

$$\boldsymbol{W} \triangleq \alpha \boldsymbol{v}_g \boldsymbol{u}_f^* \tag{7a}$$

$$\boldsymbol{a} \triangleq \beta \boldsymbol{v}_f \tag{7b}$$

$$\boldsymbol{b} \triangleq \gamma \boldsymbol{u}_g \tag{7c}$$

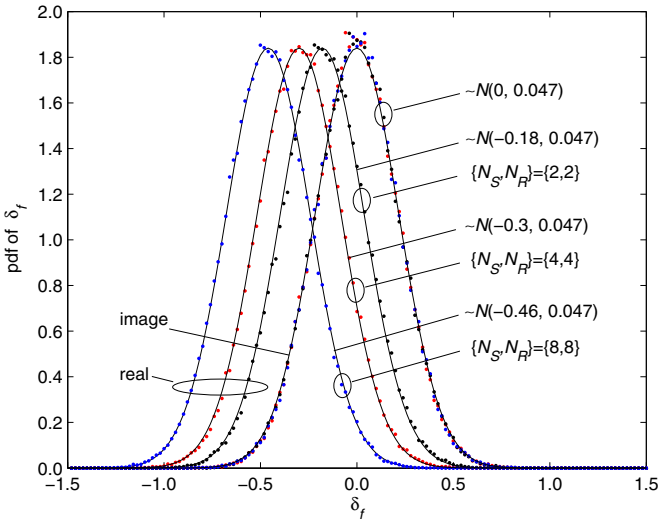

Fig. 2. Probability density function (pdf) of Gaussian random variables (illustrated line) and that of δ_f (illustrated dots) when $N_S = N_R = \{2, 4, 8\}$.

where $\boldsymbol{u}_f^*$ and $\boldsymbol{v}_f$ are the left and the right singular vectors, respectively, corresponding the largest singular value σ_h of $\boldsymbol{F}$; and $\boldsymbol{u}_g^*$ and $\boldsymbol{v}_g$ are the left and the right singular vectors, respectively, corresponding the largest singular value σ_g of $\boldsymbol{G}$. Here, α, β, and γ are used as power control factors. Now, we design the power control factors α, β, and γ for the relay, the source, and the destination, respectively. Here, we assume that the required channel information can be estimated by training sequences and fed back via a broadcasting feedback channel. In practice, estimates of the channel matrices, $\hat{\boldsymbol{F}}$ and $\hat{\boldsymbol{G}}$, should be available instead of $\boldsymbol{F}$ and $\boldsymbol{G}$. The estimated channel matrices are represented as

$$\begin{aligned} \hat{\boldsymbol{F}} &= \boldsymbol{F} + \boldsymbol{\Delta}_f \\ \hat{\boldsymbol{G}} &= \boldsymbol{G} + \boldsymbol{\Delta}_g \end{aligned} \tag{8}$$

where $\boldsymbol{\Delta}_f$ and $\boldsymbol{\Delta}_g$ are channel estimation error matrices consisting of independent zero-mean Gaussian random variables with variances $\sigma_{\Delta_f}^2$ and $\sigma_{\Delta_g}^2$, respectively. This model is valid when the orthogonal pilot sequences are used for channel estimation [11]. Accordingly, using (7) and (8) in the overall signal model (6), the received signal model is given by

$$\begin{aligned} \hat{d} &= \gamma \boldsymbol{u}_{g,1}^*(\hat{\boldsymbol{G}} - \boldsymbol{\Delta}_g)\alpha \boldsymbol{v}_{g,1}\boldsymbol{u}_{f,1}^*(\hat{\boldsymbol{F}} - \boldsymbol{\Delta}_f)\beta \boldsymbol{v}_{f,1}d \\ &\quad + \gamma \boldsymbol{u}_{g,1}^*(\hat{\boldsymbol{G}} - \boldsymbol{\Delta}_g)\alpha \boldsymbol{v}_{g,1}\boldsymbol{u}_{f,1}^*\boldsymbol{n}_s + \gamma \boldsymbol{u}_{g,1}^*\boldsymbol{n}_x \\ &= \alpha\beta\gamma(\boldsymbol{u}_{g,1}^*\hat{\boldsymbol{G}}\boldsymbol{v}_{g,1} - \boldsymbol{u}_{g,1}^*\boldsymbol{\Delta}_g\boldsymbol{v}_{g,1}) \\ &\quad \times (\boldsymbol{u}_{f,1}^*\hat{\boldsymbol{F}}\boldsymbol{v}_{f,1} - \boldsymbol{u}_{f,1}^*\boldsymbol{\Delta}_f\boldsymbol{v}_{f,1})d \\ &\quad + \alpha\gamma(\boldsymbol{u}_{g,1}^*\hat{\boldsymbol{G}}\boldsymbol{v}_{g,1} - \boldsymbol{u}_{g,1}^*\boldsymbol{\Delta}_g\boldsymbol{v}_{g,1})\boldsymbol{u}_{f,1}^*\boldsymbol{n}_s + \gamma \boldsymbol{u}_{g,1}^*\boldsymbol{n}_x \\ &= \alpha\beta\gamma(\hat{\sigma}_{f,1} + \delta_f)(\hat{\sigma}_{g,1} + \delta_g)d + \alpha\gamma(\hat{\sigma}_{g,1} + \delta_g)n_s + \gamma n_x \end{aligned} \tag{9}$$

where $\hat{\sigma}_{f,1}$ and $\hat{\sigma}_{g,1}$ are the largest singular values of $\hat{\boldsymbol{F}}$ and $\hat{\boldsymbol{G}}$, respectively, obtained from the estimated beamforming vectors and relay processing matrix; the singular value distortion factors $\delta_f = -\boldsymbol{u}_{f,1}^*\boldsymbol{\Delta}_f\boldsymbol{v}_{f,1}$ and $\delta_g = -\boldsymbol{u}_{g,1}^*\boldsymbol{\Delta}_g\boldsymbol{v}_{g,1}$; and the

978-1-4244-4148-8/09/$25.00 ©2009
This full text paper was peer reviewed at the direction of IEEE Communications Society subject matter experts for publication in the IEEE "GLOBECOM" 2009 proceedings.

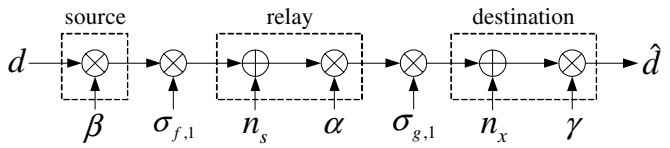

Fig. 3. Equivalent SISO system model with source-destination beamforming and relaying.

equivalent AWGN $n_s = \hat{\boldsymbol{u}}_{f,1}^* \boldsymbol{n}_s$ and $n_x = \hat{\boldsymbol{u}}_{g,1}^* \boldsymbol{n}_x$. Note that δ_f and δ_g can be modeled as complex Gaussian random variables from the fact that singular vectors are orthonormal and finite sum of independent normal random variables is normally distributed. Figure 2 illustrates the probability density function (pdf) of Gaussian random variable and δ_f by line and dots, respectively, when $N_S = N_R = \{2, 4, 8\}$. In this figure, we can see that pdf of δ_f matches well with that of Gaussian random variable. Similarly, n_s and n_x in (9) have the same variances $\sigma_{n_s}^2$ and $\sigma_{n_x}^2$ as $\boldsymbol{n}_s$ and $\boldsymbol{n}_x$. From (9), the MIMO channel model can be equivalently represented as SISO signal and channel model including source-destination beamforming and relaying as shown in Fig. 3. In order to compensate for the expected degradation in performance, we design the power control factors α, β, and γ in (9) with the estimated and given CSIs in next section.

IV. MMSE Problem Formulation

In this section, we aim for jointly designing the power control factors $\{\alpha, \beta, \gamma\}$ in order to minimize MSE under CSI uncertain condition. For the power allocation, local and global constraints are included in MMSE formulation.

A. Local Inequality Power Constraints

Local inequality power constraints are considered first. In this case, the transmit power of the source and the relay signals are limited by P_S and P_R, respectively and independently. The desired MMSE problem is then

$$\boxed{\begin{array}{l} \arg \min\limits_{\{\alpha,\beta,\gamma\}} \mathrm{E}\,|d - \hat{d}|^2 \\ \text{s.t. } \mathrm{E}\,\|\boldsymbol{s}\|^2 \le P_S \text{ and } \mathrm{E}\,\|\boldsymbol{x}\|^2 \le P_R \end{array}} \tag{10}$$

The minimization problem (10) with three inequality constraints can be transformed into

$$\arg \min_{\{\alpha,\beta,\gamma,\lambda_S,\lambda_R\}} J_L$$

where

$$J_L = \mathrm{E}\,|d - \hat{d}|^2 + \lambda_S \left(\mathrm{E}\,\|\boldsymbol{s}\|^2 - P_S\right) + \lambda_R \left(\mathrm{E}\,\|\boldsymbol{x}\|^2 - P_R\right). \tag{11}$$

Here, λ_S and λ_R are non-negative Lagrange multipliers. By substituting (7) and (9) into (11), we can derive

$$\begin{aligned} J_L = 1 &- 2\alpha\beta\gamma\hat{\sigma}_{g,1}\hat{\sigma}_{f,1} + \alpha^2\beta^2\gamma^2\bar{\sigma}_{g,1}^2\bar{\sigma}_{f,1}^2 \\ &+ \alpha^2\gamma^2\sigma_{n_s}^2\bar{\sigma}_{g,1}^2 + \gamma^2\sigma_{n_x}^2 + \lambda_S\left(\beta^2 - P_S\right) \\ &+ \lambda_R\left(\alpha^2\beta^2\bar{\sigma}_{f,1}^2 + \alpha^2\sigma_{n_s}^2 - P_R\right). \end{aligned} \tag{12}$$

TABLE I
MMSE Design under Local Inequality Power Constraints

Step 1:	Initialization, $k = 0$
	$\beta_0 = \gamma_0 = 1$, $\lambda_S = \lambda_R = 1$, $J_{L,0} = 0$.
Step 2:	Iteration: $k \leftarrow k + 1$
	$\alpha_k = f_\alpha(\beta_{k-1}, \gamma_{k-1}, \lambda_R)$ in (14a)
	$\beta_k = f_\beta(\alpha_k, \gamma_{k-1}, \lambda_S, \lambda_R)$ in (14b)
	$\gamma_k = f_\gamma(\alpha_k, \beta_k)$ in (14c)
	$\lambda_R = f_{\lambda_R}(\beta_k, \gamma_k)$ in (15a)
	$\lambda_S = f_{\lambda_S}(\alpha_k, \gamma_k, \lambda_R)$ in (15b)
	$J_{L,k} = f_{J_L}(\alpha_k, \beta_k, \gamma_k, \lambda_S, \lambda_R)$ in (11)
Step 3:	If $0 \le J_{L,k-1} - J_{L,k} \le \epsilon$ go to Step 4 and stop, otherwise go back Step 2.
Step 4:	$\boldsymbol{a} = \beta_k \boldsymbol{v}_{f,1}$; $\boldsymbol{b} = \gamma_k \boldsymbol{u}_{g,1}$; $\boldsymbol{W} = \alpha_k \boldsymbol{v}_{g,1}\boldsymbol{u}_{f,1}^*$.

where the corrupted singular values are

$$\begin{aligned} \bar{\sigma}_{f,1}^2 &= \hat{\sigma}_{f,1}^2 + 2\hat{\sigma}_{f,1}\,\mathrm{E}(\mathrm{Re}(\delta_f)) + \mathrm{E}(|\delta_f|^2) \\ \bar{\sigma}_{g,1}^2 &= \hat{\sigma}_{g,1}^2 + 2\hat{\sigma}_{g,1}\,\mathrm{E}(\mathrm{Re}(\delta_g)) + \mathrm{E}(|\delta_g|^2). \end{aligned} \tag{13}$$

Although J_L in (12) is not guaranteed to be jointly convex over all the variables $\{\alpha, \beta, \gamma\}$, it is obviously convex over each of the variables. Therefore, alternating minimization procedures, where variables are optimized one at a time while keeping all others fixed [7], [8], are applicable to get a feasible local optimal solution. Equating the derivatives of J_L in (12) with respect to α, β, and γ to zero (KKT condition [9]), we can get the optimal local power control factors as

$$\alpha = \frac{\beta\gamma\hat{\sigma}_{g,1}\hat{\sigma}_{f,1}}{\left(\gamma^2\bar{\sigma}_{g,1}^2 + \lambda_R\right)\left(\beta^2\bar{\sigma}_{f,1}^2 + \sigma_{n_s}^2\right)} \tag{14a}$$

$$\beta = \frac{\alpha\gamma\hat{\sigma}_{g,1}\hat{\sigma}_{f,1}}{\left(\alpha^2\gamma^2\bar{\sigma}_{g,1}^2\bar{\sigma}_{f,1}^2 + \lambda_R\alpha^2\bar{\sigma}_{f,1}^2 + \lambda_S\right)} \tag{14b}$$

$$\gamma = \frac{\alpha\beta\hat{\sigma}_{g,1}\hat{\sigma}_{f,1}}{\left(\alpha^2\beta^2\bar{\sigma}_{g,1}^2\bar{\sigma}_{f,1}^2 + \alpha^2\sigma_{n_s}^2\bar{\sigma}_{g,1}^2 + \sigma_{n_x}^2\right)} \tag{14c}$$

Besides, equating the derivatives of J_L in (12) with respect to λ_R and λ_S to zero and substituting (14a) and (14b), respectively, we get

$$\lambda_R = \left(\frac{\beta\gamma\hat{\sigma}_{g,1}\hat{\sigma}_{f,1}}{\sqrt{P_R\left(\beta^2\bar{\sigma}_{f,1}^2 + \sigma_{n_s}^2\right)}} - \gamma^2\bar{\sigma}_{g,1}^2\right)^+ \tag{15a}$$

$$\lambda_S = \left(\frac{\alpha\gamma\hat{\sigma}_{g,1}\hat{\sigma}_{f,1}}{\sqrt{P_S}} - \alpha^2\bar{\sigma}_{f,1}^2\left(\gamma^2\bar{\sigma}_{g,1}^2 + \lambda_R\right)\right)^+ \tag{15b}$$

where $(q)^+ = \max(0, q)$. Since the optimum values in (14) and (15) are functions of one another, it can be achieved by an iterative procedure where variables are computed one at a time keeping all others fixed [8]. At the kth iteration, denoting the MSE and the power control factors by $J_{L,k}$ and $\{\alpha_k, \beta_k, \gamma_k\}$, respectively, the proposed iterative algorithm is described in Table I. In each iterative step in Tables I, the MSE, $J_{L,k}$, is monotonically diminishing. It is also obvious that $J_{L,k}$ is

978-1-4244-4148-8/09/$25.00 ©2009

lower bounded by zero, and the convergence of $J_{L,k}$ is then guaranteed though the convergent point is not guaranteed for the global minimum. Therefore, the difference between $J_{L,k-1}$ and $J_{L,k}$ can be used as a stopping criterion with a positive design factor ϵ in Step 3.

B. Global Inequality Power Constraint

We now consider a global inequality power constraint whereby the network power, i.e., the sum of transmit power at the source and the relay nodes, is limited by P_T, where $P_T = P_S + P_R$. Accordingly, the MMSE problem (10) is modified to

$$\boxed{\begin{array}{l}\arg \min\limits_{\{\alpha,\beta,\gamma\}} \mathrm{E}\,|d-\hat{d}|^2 \\ \text{s.t. } \mathrm{E}\,\|\boldsymbol{s}\|^2 + \mathrm{E}\,\|\boldsymbol{x}\|^2 \le P_T\end{array}} \tag{16}$$

The minimization problem (16) can be transformed into

$$\arg \min_{\{\alpha,\beta,\gamma,\lambda_T\}} J_G$$

where

$$J_G = \mathrm{E}\,|d-\hat{d}|^2 + \lambda_T \left(\mathrm{E}\,\|\boldsymbol{s}\|^2 + \mathrm{E}\,\|\boldsymbol{x}\|^2 - P_T\right). \tag{17}$$

Here, λ_T is non-negative Lagrange multiplier. Using (7) and (9) in (17) yields

$$\begin{aligned} J_G = 1 &- 2\alpha\beta\gamma\hat{\sigma}_{g,1}\hat{\sigma}_{f,1} + \alpha^2\beta^2\gamma^2\bar{\sigma}^2_{g,1}\bar{\sigma}^2_{f,1} + \alpha^2\gamma^2\sigma^2_{n_s}\bar{\sigma}^2_{g,1} \\ &+ \gamma^2\sigma^2_{n_x} + \lambda_T\left(\beta^2 + \alpha^2\beta^2\bar{\sigma}^2_{f,1} + \alpha^2\sigma^2_{n_s} - P_T\right). \end{aligned} \tag{18}$$

Equating the derivatives of J_G in (18) with respect to α, β, and γ to zeros, we can get the optimal global power control factors as

$$\alpha = \frac{\beta\gamma\hat{\sigma}_{g,1}\hat{\sigma}_{f,1}}{\left(\gamma^2\bar{\sigma}^2_{g,1} + \lambda_T\right)\left(\beta^2\bar{\sigma}^2_{f,1} + \sigma^2_{n_s}\right)} \tag{19a}$$

$$\beta = \frac{\alpha\gamma\hat{\sigma}_{g,1}\hat{\sigma}_{f,1}}{\left(\alpha^2\gamma^2\bar{\sigma}^2_{g,1}\bar{\sigma}^2_{f,1} + \lambda_T\alpha^2\bar{\sigma}^2_{f,1} + \lambda_T\right)} \tag{19b}$$

$$\gamma = \frac{\alpha\beta\hat{\sigma}_{g,1}\hat{\sigma}_{f,1}}{\left(\alpha^2\beta^2\bar{\sigma}^2_{g,1}\bar{\sigma}^2_{f,1} + \alpha^2\sigma^2_{n_s}\bar{\sigma}^2_{g,1} + \sigma^2_{n_x} + \lambda_T\right)}, \tag{19c}$$

and equating $\frac{\partial J_G}{\partial \lambda_T}$ in (18) to zero, the equality for the Lagrange multiplier λ_T is obtained as

$$P_T = \beta^2 + \alpha^2\beta^2\bar{\sigma}^2_{f,1} + \alpha^2\sigma^2_{n_s}. \tag{20}$$

By substituting α and β in (19) into (20), we arrive at a degree four polynomial equation for λ_T as

$$f(x) = p_4x^4 + p_3x^3 + p_2x^2 + p_1x + p_0 \tag{21}$$

where the polynomial p_i is shown in Appendix A. We can get the optimal Lagrange multiplier from the largest real root x of $f(x) = 0$, i.e.,

$$\lambda_T = (x)^+. \tag{22}$$

Consequently, the iterative algorithm to achieve the optimal beamforming vector and relay processing matrix under the global inequality power constraint is described in Table II.

TABLE II
MMSE DESIGN UNDER GLOBAL INEQUALITY POWER CONSTRAINT

Step 1:	Initialization, $k = 0$
	$\beta_0 = \gamma_0 = 1$, $\lambda_T = 1$, $J_{G,0} = 0$.
Step 2:	Iteration: $k \leftarrow k + 1$
	$\alpha_k = f_\alpha\left(\beta_{k-1}, \gamma_{k-1}, \lambda_T\right)$ in (19a)
	$\beta_k = f_\beta\left(\alpha_k, \gamma_{k-1}, \lambda_T\right)$ in (19b)
	$\gamma_k = f_\gamma\left(\alpha_k, \beta_k, \lambda_T\right)$ in (19c)
	$\lambda_T = (x)^+$,
	where x is the largest real root satisfying (20)
	$J_{G,k} = f_{J_G}\left(\alpha_k, \beta_k, \gamma_k, \lambda_T\right)$ in (11)
Step 3:	If $0 \le J_{G,k-1} - J_{G,k} \le \epsilon$ go to Step 4 and stop,
	otherwise go back Step 2.
Step 4:	$\boldsymbol{a} = \beta_k\boldsymbol{v}_{f,1}$; $\boldsymbol{b} = \gamma_k\boldsymbol{u}_{g,1}$; $\boldsymbol{W} = \alpha_k\boldsymbol{v}_{g,1}\boldsymbol{u}^*_{f,1}$.

V. SIMULATION AND DISCUSSION

In this section, computer simulations are conducted to examine the BER performance of the designed systems. The transmitted signals from the sources are modulated by quadrature phase-shift keying (QPSK) or 16-quadrature amplitude modulation (QAM), and the modulated symbols are grouped into frames consisting of 100 symbols. For each frame, flat fading MIMO channel matrices $\boldsymbol{F}$ and $\boldsymbol{G}$ are generated from independent Gaussian random variables with zero mean and unit variance. Channels $\boldsymbol{F}$ and $\boldsymbol{G}$ are fixed during a frame, but they vary independently over frames. The results shown below are the averages over 10^5 independent trials. The power limits are assumed to be $P_S = P_R = 1$ and $P_T = 2$. For simulation, the received SNRs at the relay and destination nodes are defined as

$$\mathrm{SNR}_{RS} \triangleq \frac{P_S}{\sigma^2_{n_s}}$$

$$\mathrm{SNR}_{DR} \triangleq \frac{P_R}{\sigma^2_{n_x}},$$

respectively. The SNR_{RS} is set to 25 dB and BER performance is evaluated over SNR_{DR}.

In Fig. 4, the BER performance under local and global power constraints are examined when CSIs are perfect. Figures 4(a) and (b) show the BER performances when QPSK and 16-QAM symbols are transmitted, respectively. As expected, the performance of the global power control system is better than that of the local power control system since the different effective SNRs at the relay and the destination nodes can be adjusted. In other word, a relatively low SNR, which is a bottleneck in the network performance, can be increased at the expense of a relatively high SNR, resulting in performance improvement. In our simulation, we use $\epsilon = 10^{-4}$ and observe that the average number of required iteration is around 30 in Tables I and II.

To determine the modified power control factors in (14) and (19), the corrupted singular values $\bar{\sigma}^2_{f,1}$ and $\bar{\sigma}^2_{g,1}$ in (13) are required at each node. Considering up to 10% channel

978-1-4244-4148-8/09/$25.00 ©2009

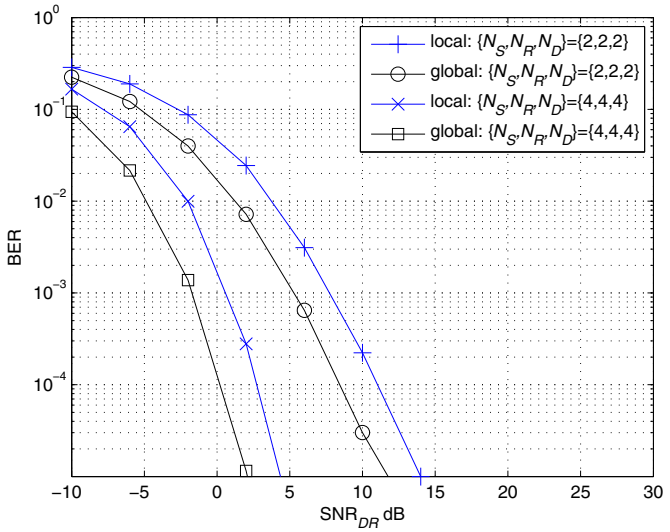

(a)

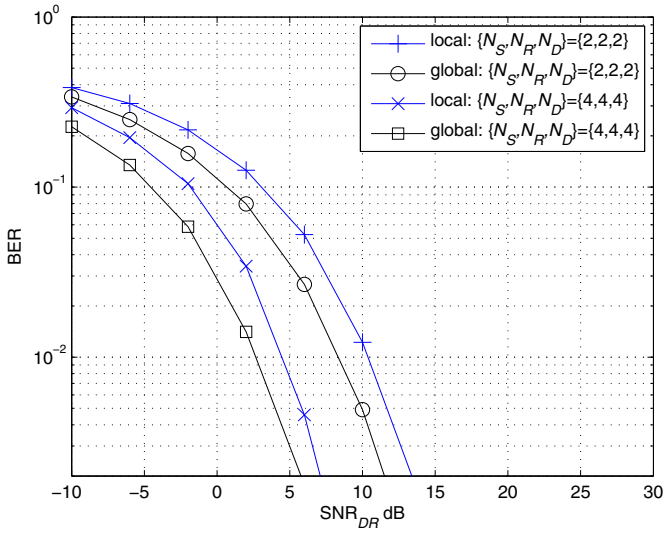

(b)

Fig. 4. BER performance when the CSIs are perfect and $\mathrm{SNR}_{RS} = 25$ dB. (a) QPSK. (b) 16-QAM.

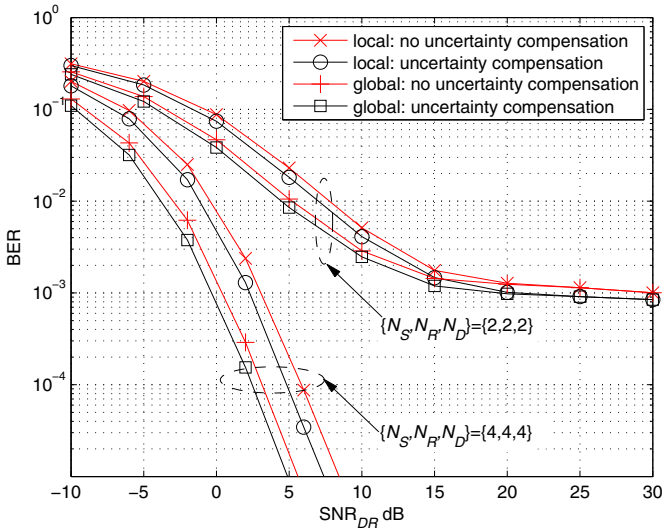

(a)

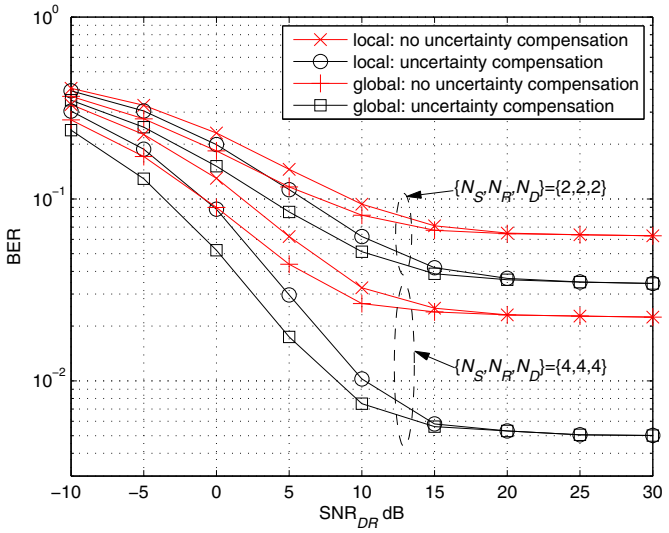

(b)

Fig. 5. BER comparison of the channel uncertainty compensation schemes and no compensation schemes when $\mathrm{SNR}_{RS} = 25$ dB and $\sigma^2_{\Delta_f} = \sigma^2_{\Delta_g} = 0.1$. (a) QPSK. (b) 16-QAM.

uncertainty, i.e., $\sigma^2_{\Delta_f} \leq 0.1$ and $\sigma^2_{\Delta_g} \leq 0.1$, the following model is used to obtain $\bar{\sigma}^2_{f,1}$ and $\bar{\sigma}^2_{g,1}$:

$$\begin{aligned} \mathrm{E}(\mathrm{Re}(\delta_f)) &\approx (a_2\sigma^2_{\Delta_f} + a_1)\sigma^2_{\Delta_f} \\ \mathrm{E}(|\delta_f|^2) &\approx (b_2\sigma^2_{\Delta_f} + b_1)\sigma^2_{\Delta_f} \\ \mathrm{E}(\mathrm{Re}(\delta_g)) &\approx (a_2\sigma^2_{\Delta_g} + a_1)\sigma^2_{\Delta_g} \\ \mathrm{E}(|\delta_g|^2) &\approx (b_2\sigma^2_{\Delta_g} + b_1)\sigma^2_{\Delta_g} \end{aligned} \tag{23}$$

In (23), the coefficients $\{a_i, b_i\}$ are numerically obtained from the polynomial fitting method [9] to achieve a normalized MSE (NMSE) that is less than 10^{-5} (see Appendix B).

Figure 5 illustrates the BER performance network under CSI uncertainty. The 10% channel uncertainty is modeled as white Gaussian noise and added to the original channel values, i.e., the variances of the errors are chosen as $\sigma^2_{\Delta_f} = 0.1$, and $\sigma^2_{\Delta_g} = 0.1$. For the comparison purpose, the results without considering CSI uncertainty are included. These results can be obtained by assuming $\delta_f = \delta_g = 0$ in our solutions. The uncertainty compensation effect is negligible in Fig. 5(a) when QPSK modulation is used, since in this case the detection performance is robust against the signal power. While when 16-QAM is used, we can see the noticeable performance gap in Fig. 5(b). Note that the performance gap between the local and global power control methods is negligible in the region where SNR_{DR} is similar to SNR_{RS}, i.e., $20\,\mathrm{dB} \leq \mathrm{SNR}_{DR} \leq 30\,\mathrm{dB}$. Furthermore, it can be seen that the approximation in (23) works favorably.

978-1-4244-4148-8/09/$25.00 ©2009

VI. Conclusion

In this paper, we designed the power control factors for MMSE-based beamforming and relay processing under CSI uncertainties. Local and global inequality power constraints on the source and the relay nodes are considered in MMSE formulation. Simulation results show that the effect of channel uncertainties on system performance and the proposed power control factors make the system more robust against channel uncertainties.

Appendix A
The Polynomial Coefficients in (21)

The coefficients of the polynomial p_i in (21) are given by

$$
\begin{aligned}
p_4 &= P_T v_3^2 v_5 \\
p_3 &= 2P_T v_3 v_5 (v_3 v_4 + v_6) \\
p_2 &= P_T v_5 (v_3^2 v_4^2 + 4 v_3 v_4 v_6 + v_6^2) - (v_1 v_5 + \sigma_{n_s}^2 v_2 v_3^2) \\
p_1 &= 2P_T v_4 v_5 v_6 (v_3 v_4 + v_6) - 2 v_1 v_4 v_5 - 2\sigma_{n_s}^2 v_2 v_3 v_6 \\
p_0 &= P_T v_4^2 v_5 v_6^2 - v_1 v_4^2 v_5 - v_1 v_2 \bar{\sigma}_{f,1}^2 - \sigma_{n_s}^2 v_2 v_6^2
\end{aligned}
$$

where

$$
\begin{aligned}
v_1 &= \hat{\bar{\alpha}}^2 \hat{\bar{\gamma}}^2 \hat{\sigma}_{g,1}^2 \hat{\sigma}_{f,1}^2 \\
v_2 &= \hat{\bar{\beta}}^2 \hat{\bar{\gamma}}^2 \hat{\sigma}_{g,1}^2 \hat{\sigma}_{f,1}^2 \\
v_3 &= \hat{\bar{\alpha}}^2 \bar{\sigma}_{f,1}^2 + 1 \\
v_4 &= \hat{\bar{\gamma}}^2 \bar{\sigma}_{g,1}^2 \\
v_5 &= (\hat{\bar{\beta}}^2 \bar{\sigma}_{f,1}^2 + \sigma_{n_s}^2)^2 \\
v_6 &= \hat{\bar{\alpha}}^2 \hat{\bar{\gamma}}^2 \bar{\sigma}_{g,1}^2 \bar{\sigma}_{f,1}^2 .
\end{aligned}
$$

Appendix B
The Polynomial Coefficients $\{a_i, b_i\}$ in (23)

According to the dimension of the channel matrix $\boldsymbol{F}$ or $\boldsymbol{G}$, the polynomial coefficients $\{a_i, b_i\}$ in (23) are given in Table III by computer simulation. In simulation, for example, the NMSEs with respect to δ_f are given by

$$
\frac{\sum \left| \mathrm{E}(\mathrm{Re}(\delta_f)) - (a_2 \sigma_{\Delta_f}^2 + a_1) \sigma_{\Delta_f}^2 \right|^2}{\sum \left| \mathrm{E}(\mathrm{Re}(\delta_f)) \right|^2}
$$

and

$$
\frac{\sum \left| \mathrm{E}(|\delta_f|^2) - (b_2 \sigma_{\Delta_f}^2 + b_1) \sigma_{\Delta_f}^2 \right|^2}{\sum \left| \mathrm{E}(|\delta_f|^2) \right|^2}
$$

where the expectations are performed over 10^6 independent channel and noise realizations.

TABLE III
Coefficients $\{a_i, b_i\}$ of approximations in (23)

Dimension	a_2	a_1	NMSE
2×1	0.5535	-1.3225	$< 10^{-5}$
2×2	0.8589	-1.8129	$< 10^{-5}$
2×3	0.9545	-2.1517	$< 10^{-6}$
2×4	0.9431	-2.4209	$< 10^{-5}$
3×1	0.6954	-1.6546	$< 10^{-6}$
3×3	1.0756	-2.5063	$< 10^{-5}$
3×4	1.1859	-2.7891	$< 10^{-5}$
4×1	0.8270	-1.9326	$< 10^{-5}$
4×4	1.3062	-3.0798	$< 10^{-5}$
Dimension	b_2	b_1	NMSE
2×1	0.8975	1.0019	$< 10^{-6}$
2×2	2.0624	1.0255	$< 10^{-5}$
2×3	3.2781	1.0287	$< 10^{-6}$
2×4	4.3784	1.0391	$< 10^{-6}$
3×1	1.7325	1.0099	$< 10^{-6}$
3×3	4.7669	1.0311	$< 10^{-6}$
3×4	5.9402	1.0551	$< 10^{-5}$
4×1	2.4589	1.0318	$< 10^{-5}$
4×4	7.4055	1.0666	$< 10^{-5}$

References

[1] N. Khajehnouri and A. H. Sayed, "Distributed MMSE relay strategies for wireless sensor networks," *IEEE Trans. Signal Processing*, vol. 55, pp. 3336–3348, Jul. 2007.

[2] Y. Li, B. Vucetic, Z. Zhow, and M. Dohler, "Distributed adaptive power allocation for wireless relay networks," *IEEE Trans. Wireless Commun.*, vol. 6, pp. 948–958, Mar. 2007.

[3] Y. Zhao, R. Adve, and T. J. Lim, "Improving amplify-and-forward relay networks: Optimal power allocation versus selection," *IEEE Trans. Wireless Commun.*, vol. 6, pp. 3114–3123, Mar. 2007.

[4] D. Veronesi and N. Benvenuto, "Minimum sum-power design of a cooperative system using the amplify and forward protocol," in *Proc. IEEE International Conference on Signal Processing and Communications (ICSPC)*, Dubai, United Arab Emirates, Nov. 2007, pp. 1159–1162.

[5] S. W. Peters and R. W. Heath Jr., "Nonregenerative MIMO relaying with optimal transmit antenna selection," *IEEE Signal Processing Lett.*, vol. 15, pp. 421–424, 2008.

[6] B. Khoshnevis, W. Yu, and R. Adve, "Grassmannian beamforming for MIMO amplify-and-forward relaying," *IEEE J. Select. Areas Commun.*, vol. 26, pp. 1397–1407, Oct. 2008.

[7] D. Bertsekas and J. Tsitsiklis, *Parallel and Distributed Computation*, Englewood Cliffs, NJ: Prentice-Hall, 1989.

[8] J. Joung and Y. H. Lee, "Regularized channel diagonalization for multiuser MIMO downlink using a modified MMSE criterion," *IEEE Trans. Signal Processing*, vol. 55, pp. 1573–1579, Apr. 2007.

[9] S. Boyd and L. Vandenberghe, *Convex Optimization*. Cambridge, U.K.: Cambridge Univ. Press, 2004.

[10] J. Joung and A. H. Sayed, "Design of half-and full-duplex relay systems based on the MMSE formulation," in *IEEE Workshop on Statittical Signal Processing (SSP),* Wales, UK, Aug–Sept. 2009.

[11] A. F. Naguib, V. Tarokh, N. Seshadri, and A. R. Calderbank, "A space-time coding modem for high-data-rate wireless communications," *IEEE J. Select. Areas Commun.,* vol. 16, pp. 1459–1478, Oct. 1998.

978-1-4244-4148-8/09/$25.00 ©2009